

Time- and Energy-Resolved Mass Spectroscopy: The Condensed Vacuum Discharge between Solid Electrodes

J. FRANZEN and K. D. SCHUY

Max-Planck-Institut für Chemie (Otto-Hahn-Institut) (Abteilung Massenspektroskopie), Mainz

(Z. Naturforschg. **20 a**, 176—180 [1965]; eingegangen am 14. November 1964)

A method is described to obtain time- and energy-resolved mass spectra of ions from discharges between solid electrodes in vacuum. The method is used to investigate the triggered condensed discharge. The discharge is found to consist of two distinct phases: a short high-voltage breakdown (spark) is followed by a longer low-voltage discharge (arc). A model is proposed to explain the processes involved.

In addition to the conventional r. f. DEMPSTER spark ion source, a number of ion sources based on other discharge types between electrodes in vacuum have recently been suggested for the quantitative mass spectroscopic analysis of solids. However, up to now little is known concerning the physical processes leading to ion formation. To obtain some insight into the processes occurring in discharges in vacuum, it is necessary to investigate the time variation of the yield of individual ion species as they emerge from the discharge.

1. Time-Resolved Mass Spectroscopy

We have developed a method of time-resolved mass spectroscopy for the investigation of ion formation processes in vacuum. The basic principle is shown in Fig. 1. Ions emerging from the source are accelerated to an ion beam by an ion optical lens system in the usual manner. Prior to its passage through the object slit of the mass spectrograph, the

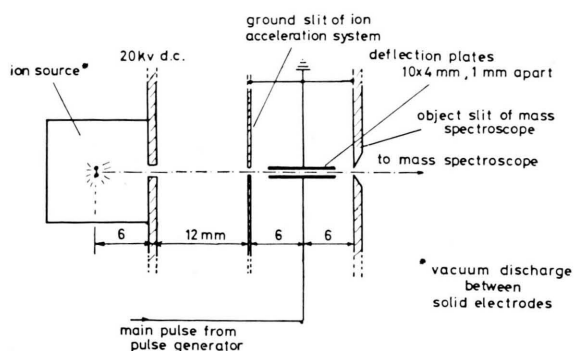


Fig. 1. Geometry of ion source and accelerating system with deflection plates. The ion source indicated in the figure is a thyratron-triggered condensed discharge between solid electrodes in vacuum.

ion beam passes a pair of deflection plates mounted between the final grounded slit of the ion accelerating system and the object slit of the mass spectrograph. A potential in the order of 100 v is applied to the deflection plates such that the ion beam is sufficiently deflected away from the object slit: the beam cannot enter the mass analyzer. At a pre-determined instant after the initiation of the ion formation process, the deflection plates can be grounded for a selected time interval. During this interval, the ion beam is not deflected. It passes the object slit of the mass spectrograph and is analyzed.

To experimentally demonstrate time-resolution, we used a Solartron type GO 1005 Decade Pulse Generator with two outputs. A pre-pulse (see Fig. 2) triggers the ignition of the discharge between the electrodes. The main pulse is directly fed to the deflection plates. The delay time t_{del} of the main pulse with respect to the pre-pulse as well as the length of the main pulse can be adjusted arbitrarily. Time-resolution is better than 200 ns. The reproducibility of the delay time setting of the main pulse is better than 50 ns.

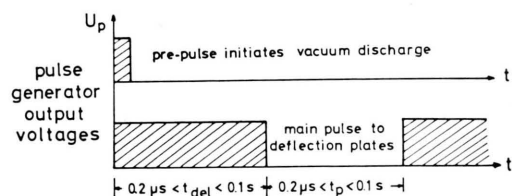


Fig. 2. Schematic representation of Solartron Type GO 1005 decade pulse generator outputs as used for time-resolved mass spectroscopy.

The arrangement of the deflection plates in front of the object slit of the mass spectrograph offers two distinct advantages: it allows ion beam manipulation



Dieses Werk wurde im Jahr 2013 vom Verlag Zeitschrift für Naturforschung in Zusammenarbeit mit der Max-Planck-Gesellschaft zur Förderung der Wissenschaften e.V. digitalisiert und unter folgender Lizenz veröffentlicht: Creative Commons Namensnennung-Keine Bearbeitung 3.0 Deutschland Lizenz.

Zum 01.01.2015 ist eine Anpassung der Lizenzbedingungen (Entfall der Creative Commons Lizenzbedingung „Keine Bearbeitung“) beabsichtigt, um eine Nachnutzung auch im Rahmen zukünftiger wissenschaftlicher Nutzungsformen zu ermöglichen.

This work has been digitalized and published in 2013 by Verlag Zeitschrift für Naturforschung in cooperation with the Max Planck Society for the Advancement of Science under a Creative Commons Attribution-NoDerivs 3.0 Germany License.

On 01.01.2015 it is planned to change the License Conditions (the removal of the Creative Commons License condition "no derivative works"). This is to allow reuse in the area of future scientific usage.

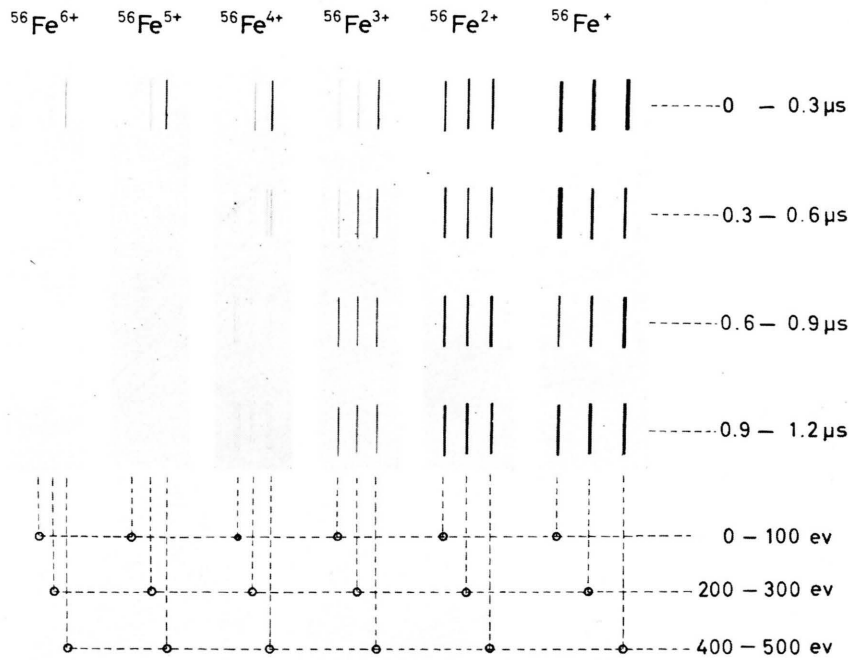


Fig. 4. Some portions of mass spectra displaying the lines of singly and multiply charged iron ions from various phases of the triggered condensed discharge.

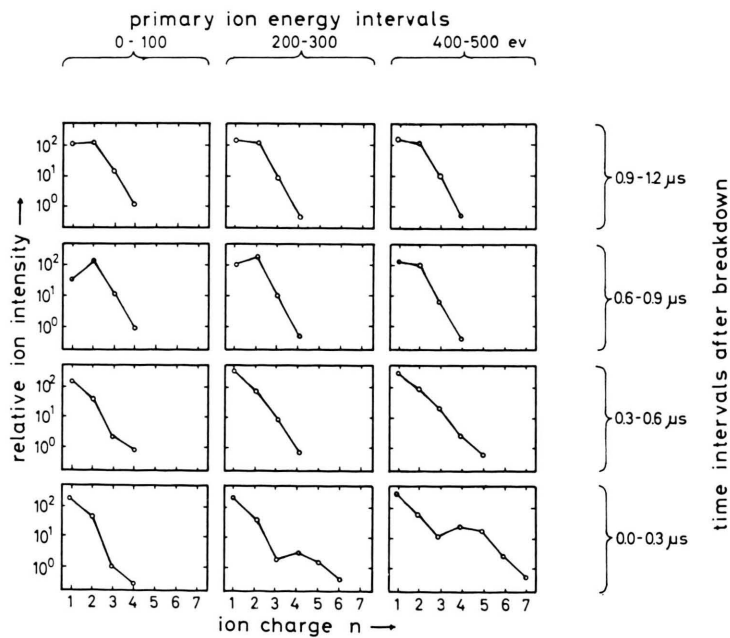


Fig. 5. Photometric evaluation of lines shown in Fig. 4: energy- and time-resolved abundance distributions of iron among its ionization states, from stainless steel mass spectra. Arbitrary units are used for each exposure.

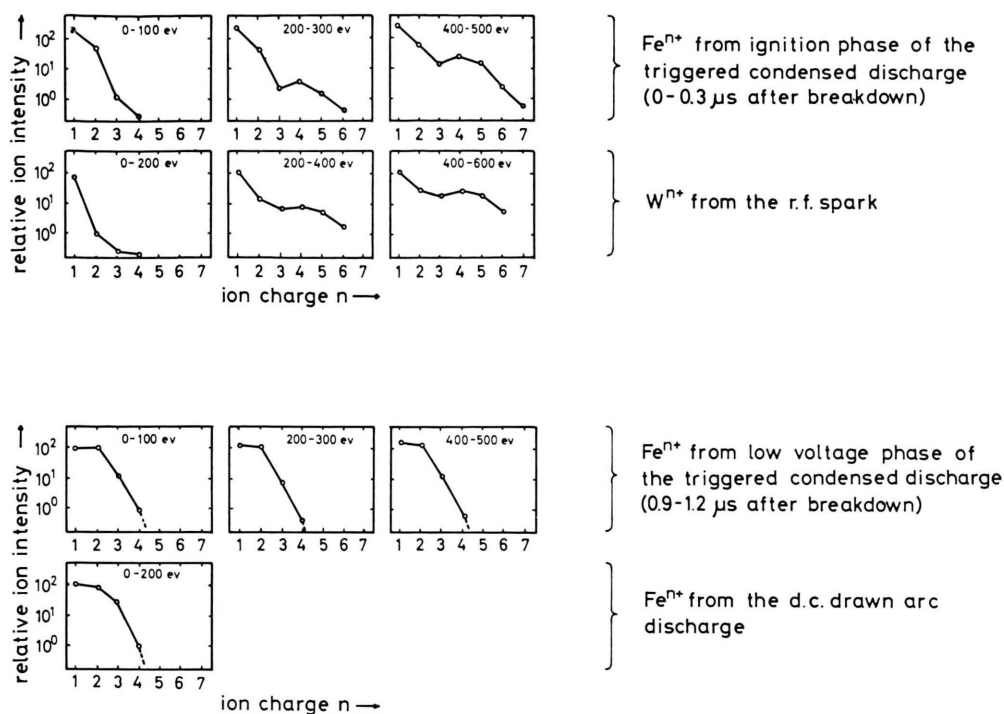
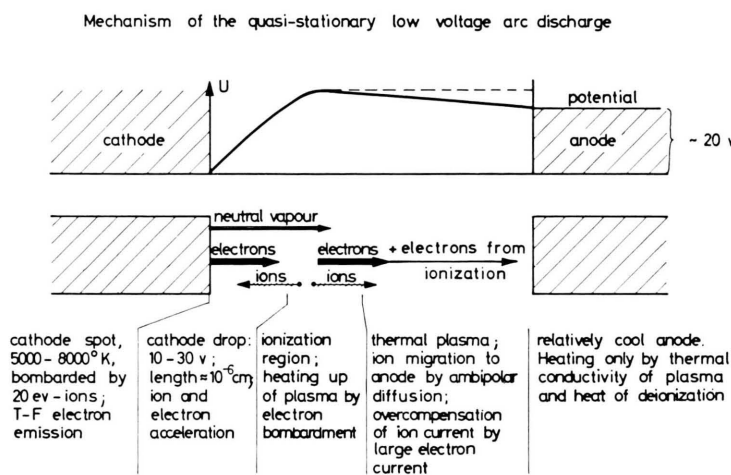


Fig. 6. Comparison of the triggered condensed discharge with the r. f. spark and the d. c. drawn arc, respectively. Abundance distributions among the ionization states of ions originated within different time phases of the triggered condensed discharge are compared with those of the r. f. spark and the d. c. drawn arc. Arbitrary units are used for each curve.



Plasma column probably formed by vapour pressure and magnetohydrodynamic forces.

Fig. 7. Proposed qualitative model of the low-voltage arc discharge mechanism. Ions are preferentially formed from cathode material.

without interfering with the ion optical properties of the instrument, and it keeps small the times of flight of the ions from their point of origin to the deflection plates, thus reducing mass and energy discrimination.

The time of flight required by an ion of mass m and initial energy E_0 to traverse the distance from its point of origin to the deflection plates is determined by the applied ion accelerating potential and the source geometry. Some typical figures are given in Table 1 for ions accelerated to 20 kev in the source configuration shown in Fig. 1. For ion formation

$\frac{E_0}{m}$	0.1 ev	1 ev	10 ev	100 ev	1000 ev
10 u	4.37	1.42	0.48	0.19	0.08 μ s
20 u	6.19	2.00	0.68	0.25	0.12 μ s
40 u	8.74	2.84	0.96	0.36	0.17 μ s
100 u	13.83	4.47	1.52	0.57	0.27 μ s
200 u	19.55	6.34	2.15	0.64	0.37 μ s

Table 1. Times of flight required by ions of mass m and initial kinetic energy E_0 to traverse the distance between their point of origin and the centre of the deflection plates, after acceleration to 20 kev through the source geometry shown in Fig. 1.

processes of duration $< 0.1 \mu$ s, these different times of flight can easily be employed to measure the energy distribution of low-energy ions leaving the discharge. For longer processes, the distance between the discharge and the accelerating region can be reduced. This measure diminishes the times of flight of the ions and permits study of the variation of ion formation processes with time.

2. Energy-Resolved Ion Analysis

For ion analysis, we use a double focusing mass spectrograph of the original MATTAUCH-HERZOG geometry. Ions are detected on photographic plates in the usual manner.

In addition to time-resolving the discharge process, we energy-resolve the ions issuing from the source. An energy-resolution of about 100 ev is obtained by a narrow energy slit in front of the magnetic field of the mass spectrograph, and a small aperture in front of the radial deflection field. Ions of different primary energies are analyzed by different ratios of ion accelerating voltage to radial field voltage.

3. The Triggered Condensed Discharge

We have applied time-resolution and energy-resolution to a study of the triggered condensed discharge^{1,2} between solid electrodes in vacuum.

The discharge circuit used in our experiments is schematically shown in Fig. 3. The capacitor C_1 is charged to a few kv by a d. c. charging circuit. A hydrogen-filled thyatron, triggered by a pulse generator, acts as a fast switch to discharge the

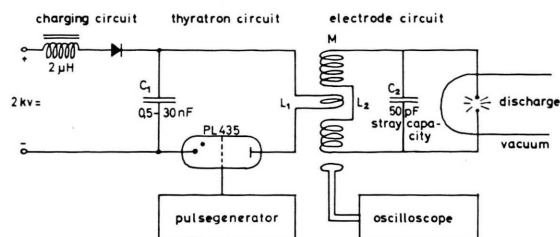


Fig. 3. Diagrammatic representation of discharge circuit.

capacitor across the primary of a pulse transformer. The fast-rise current induces a high voltage peak in the secondary of the pulse transformer, igniting a discharge between two electrodes in vacuum.

Up to the instant of ignition, oscillograms of voltage and current agree with calculations of a comparable circuit³ so that the required conditions for instantaneous and unidirectional ignition processes can be taken from this work.

The duration of gap breakdown, e. g. the time necessary for the voltage to drop from some 10^4 volts down to a few volts, is less than 10^{-7} s. Voltage and current oscillograms of the breakdown phase are very similar to those observed by one of us in the r. f. DEMPSTER spark⁴. The condensed discharge does not terminate with gap breakdown, however, due to the higher energy capacity of the circuit. After breakdown, the voltage oscillograms inoscillate with the voltage curve of the short circuit case, corresponding to a high-current, low-voltage discharge, closely resembling the voltage-time relationship of the d. c. drawn arc⁵. The duration of the low voltage discharge phase is proportional to the square root of the primary capacitance C_1 . Using a condenser C_1 of 30 nf, we obtained low-voltage

¹ R. E. HONIG, S. S. GLASS, and J. R. WOOLSTON, Conf. paper, VIth. Int. Conf. on Ionization Phenomena in Gases, Paris 1963.

² J. FRANZEN and K. D. SCHUY, Conf. paper, Reg. Meet., DPG-HMS, Bad Nauheim, Germany, April 1964.

³ D. A. SINCLAIR and R. N. WHITTEM, Spectrochim. Acta 13, 168 [1958].

⁴ J. FRANZEN and H. HINTENBERGER, Z. Naturforsch. 18 a, 397 [1963].

discharges of duration in the order of 3 μ s. HONIG and cooperators succeeded in increasing the length of the low-voltage discharge phase up to 100 μ s by suitable measures ^{1, 6}.

4. Results

The combination of both time- and energy-resolution enables us to expose a single photographic plate with ions having different primary energies, and having originated at different instants of the discharge.

Fig. 4 * shows some portions of a photographic plate, displaying the lines $^{56}\text{Fe}^+$ to $^{56}\text{Fe}^{6+}$, from mass spectra obtained with the triggered condensed discharge between iron electrodes. All exposures were made to approximately equal total charge. The exposures in the vertical show the lines of ions which originated in different time intervals from 0 to 1.2 μ s after the ignition of the thyatron. In the horizontal, ions of primary energies within the energy intervals 0–100 ev, 200–300 ev, and 400–500 ev are displayed. The thyatron was conducting for a total of 1.3 μ s.

As expected from the oscillograms, the mass spectra of ions formed during the gap breakdown phase (0 to 0.3 μ s) are very similar to those obtained with the r. f. spark ⁴. In contrast, the mass spectra of ions originating during the low-voltage phase of the discharge very much resemble those found with the d. c. drawn arc ⁷.

Fig. 5 shows the photometrically evaluated energy- and time-resolved distributions of iron on its different ionization states. The intensity values have been corrected for line width and line length as well as for photographic response. As is customary ⁸, the different photographic sensitivities for ions of different charge were corrected with the assumption that the action of ions of the same mass on the photoplate is linearly proportional to their energy and independent on their charge. It should be noted that the

mode of plotting employed in the figure does not permit the comparison of intensities for ions within different primary energy intervals or with different times of origin. For example, ions from the low-voltage phase of the discharge show a considerably smaller primary energy distribution than those which originated during the breakdown phase. In the low-voltage phase, less than 1% of the ions have energies within 200 to 300 ev, and less than 0.1% lie within the energy interval from 400 to 500 ev, relative to the 0 to 100 ev interval.

In Fig. 5, the large difference in shape between the distribution of ions from the ignition phase (0 to 0.3 μ s) and the low-voltage phase (0.6 to 1.2 μ s) is rather striking. For the low-voltage phase of the discharge, we observe a distribution of ionization states typical for a plasma in thermal equilibrium as governed by the SAHA-EGGERT equation (see below).

To emphasize the difference between the two discharge types, the ionization state distributions of the triggered condensed discharge are compared with those of the r. f. spark and of the d. c. drawn arc in Fig. 6. The close similarity between the corresponding distributions of the two high-voltage sparks * (see Fig. 6, top) and the two low-voltage arcs * (see Fig. 6, bottom) is obvious. However, some ions from the low-voltage arc phase seem to be superimposed on the low-energy ions from the ignition phase. For the d. c. drawn arc discharge, ions with primary energies higher than 200 ev could not be detected ^{9, 6}.

5. Discussion

Time- and energy-resolution of the ions from a triggered condensed discharge revealed that the total discharge process can be divided into two subsequent phases.

The ignition phase shows a high-voltage breakdown of the gap between the electrodes similar to that observed in the r. f. spark ¹⁰. The following

⁵ K. D. SCHUY and J. FRANZEN, Conf. paper, Reg. Meet., DPG-HMS, Bad Nauheim, Germany, April 1964.

⁶ R. E. HONIG, Conf. paper, XIIth Ann. Conf. on Mass Spectroscopy and Allied Topics, Montreal, June 1964.

* Fig. 4–7 see p. 176 a, b.

⁷ K. D. SCHUY and H. HINTENBERGER, Z. Naturforschg. **18a**, 926 [1963].

⁸ E. B. OWENS and N. A. GIARDINO, Anal. Chem. **35**, 1172 [1963].

* Because of its highly dynamic nature, we denote the high-voltage gap breakdown by "high-voltage spark" while we consider the low-voltage discharge as a "low-voltage arc" because of its quasi-stationary character. These expressions somewhat disagree with those customary in optical spectroscopy. There a "spark" denotes a strongly ion-forming process ("spark spectrum") while the "arc" classifies a discharge giving rise to the "arc spectrum" of neutral atoms or molecules.

⁹ K. D. SCHUY, PhD-Thesis, University of Mainz, "D 77".

breakdown mechanism is based on a model proposed by HONIG and cooperators^{11, 1, 6}.

If the field strength between the electrodes reaches an average value of about 10^5 V/cm, field electron emission commences at cathode asperities, presumably on small whiskers^{12, 13}. This pre-breakdown phase is reversible^{14, 15}. The electrons form weakly divergent beams impinging on the anode surface, heating up small areas of the surface^{16, 12}. Vaporized anode material is ionized by the electrons and increasingly fills up the gap with positive space charge. The space charge increases the field strength at the cathode surface, giving rise to increased electron emission. If the voltage across the electrodes exceeds a critical value, this auto-amplification process goes beyond the stability range of the pre-breakdown phase¹⁷. The current increases irreversibly; the voltage across the electrodes drops from some 10^4 volts to practically zero. This breakdown phase terminates within less than 10^{-7} s. In agreement with this model, extremely short discharges as obtained with small primary condensers C_1 , show that anode ions appear preferentially^{6, 2}.

Our observations do not permit conclusions to be drawn concerning the processes occurring in the transition interval between the high-voltage spark and the following low-voltage arc. It appears (see Fig. 5, time interval 0.3 to 0.6 μ s) that the duration of the transition region is in the order of 0.3 μ s. Ion emission during this period is relatively low.

For the low-voltage arc phase we propose the following model, based on the theory of particle currents in the positive column of glow discharges¹⁸ and on the theory of cathode mechanisms in vacuum arcs^{19, 20}.

Fig. 7 gives a diagrammatic view of the potential distribution and the various particle currents across the electrode gap of the low-voltage arc. The potential remains practically constant over the greater portion of the gap, and drops from about 20 v to zero within the very short cathode drop region. The

cathode drop is only about one mean free electron path wide. Due to the high pressure (some atmospheres) in this region, it somewhat resembles an electric double layer.

Ions present at the cathode drop boundary are accelerated towards the cathode. Upon impact and de-ionization, they heat up the cathode surface to form a cathode spot. From the hot cathode spot, reaching temperatures up to 6000 °K, large numbers of neutral atoms of the surface evaporate and migrate across the cathode drop. Simultaneously, electrons are drawn out of the hot cathode spot by the high field strength existing at the surface (Temperature-Field-Emission¹⁹). The electrons, accelerated in the cathode drop, heat up the vapour in the subsequent positive column by multiple collisions to form a plasma of very high temperature. The process is only operative at current densities in the order of 10^5 A/cm² (cf.²⁰), and results in high pressures in the plasma. Due to the high plasma pressure, thermal equilibrium is attained within less than 10^{-8} s (cf.^{21, 22}). The high temperature leads to an almost completely ionized plasma. According to calculations of particle currents in glow discharges¹⁸, only about half of the ions formed in the plasma are accelerated towards the cathode. The other half migrates towards the anode by ambipolar diffusion and is responsible for the net transfer of cathode material to the anode as observed experimentally. We notice that the fraction of ions migrating to the anode transfers charge in the wrong direction. However, this current of positive charge is overcompensated by a larger current of electrons freed in the plasma by ionization. The anode itself remains relatively cool in this process. It is heated only by the thermal conductivity of the plasma and by the heats of de-ionization and condensation.

According to the SAHA-EGGERT equation, the distribution of ions among their ionization states is, for a plasma in thermal equilibrium, uniquely determined by plasma temperature and electron pressure. The

¹⁰ J. FRANZEN, Z. Naturforschg. **18 a**, 410 [1963].

¹¹ R. E. HONIG, private communication.

¹² R. P. LITTLE and W. T. WHITHNEY, J. Appl. Phys. **34**, 2430, 3141 [1963].

¹³ H. E. TOMASCHKE, Coord. Science Lab. Rep. R-192, Univ. of Illinois [1964].

¹⁴ L. I. PIVOVAR and V. I. GORDIENKO, Sov. Phys.-Techn. Phys. **3**, 2101 [1958]; **7**, 908 [1963].

¹⁵ M. GOLDMAN and A. GOLDMAN, J. Phys. Radium **24**, 303 [1963].

¹⁶ D. J. DeGEETER, J. Appl. Phys. **34**, 919 [1963].

¹⁷ W. S. BOYLE, P. KISLIUK, and L. H. GERMER, J. Appl. Phys. **26**, 720 [1955].

¹⁸ W. WEIZEL, Lehrbuch der theoretischen Physik, Vol. 2, Springer-Verlag, Berlin 1952, p. 1316 ff.

¹⁹ T. H. LEE, J. Appl. Phys. **30**, 166 [1959].

²⁰ T. H. LEE and A. GREENWOOD, J. Appl. Phys. **32**, 916 [1961].

²¹ S. MANDELSTAM, Spectrochim. Acta **11**, 255 [1959].

²² H. KREMPL, Z. Phys. **167**, 302 [1962].

distributions shown in Fig. 6 both for the low-voltage arc phase and the d. c. drawn arc very much resemble such SAHA distributions. Indeed, for the d. c. drawn arc discharge we were able to compute theoretical distributions which agree with the experi-

mental distributions far better than to a factor of two²³.

Acknowledgement

We wish to express our sincere thanks to Professor HINTENBERGER for his continuous interest and encouragement.

²³ J. FRANZEN and K. D. SCHUY, in preparation.

Dissociation of Meta-stable Ions in Mass Spectrometers with Release of Internal Energy

J. H. BEYNON, R. A. SAUNDERS, and A. E. WILLIAMS

Imperial Chemical Industries Limited, Dyestuffs Division, Hexagon House, Manchester 9, England

(Z. Naturforsch. **20 a**, 180—183 [1965]; eingegangen am 25. November 1964)

Certain of the "meta-stable peaks" in mass spectra are abnormally wide. This extra width is shown to be associated with release of kinetic energy during fragmentation. Methods are presented for measuring this energy release and values are given for various transitions in the spectra of aromatic nitro compounds.

Meta-stable ions are often detected in the mass spectra of organic compounds^{1, 2}. These ions may be detected if they dissociate near the entrance slit of the magnetic analyser in sector magnetic field mass spectrometers. If ions of original mass m_1 dissociate to produce ions of mass m_2 , a peak appears in the mass spectrum at a position m^* where

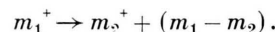
$$m^* \approx m_2^2/m_1. \quad (1)$$

These peaks are usually quite small and are much broader than peaks produced by normal stable ions. They often extend over a range of several mass numbers and usually have a shape resembling a GAUSSIAN distribution curve. Their maxima are usually sufficiently well defined to enable one to determine the values of m_1 and m_2 , from equation (1), for the ions involved in the transition. Occasionally, however, some of these "meta-stable peaks" are observed to be much broader than usual and to have a relatively flat top. Such peaks have been observed by NEWTON and SCIAMANNA corresponding to the meta-stable state of the doubly-charged carbon dioxide ion³. The length of this flat portion is found to vary inversely with the accelerating voltage. It is shown that the increased width of these peaks is caused by the release of a small amount of kinetic energy during the dissociation process.

Theoretical Considerations

In arriving at the approximate relationship of equation (1), HIPPLE and his co-workers² assumed that there was a negligible release of kinetic energy during the dissociation. In such a case the kinetic energy acquired by an ion of mass m_1 during the acceleration process is shared on dissociation between the two resulting particles in proportion to their masses.

Let us now consider an ion m_1^+ which is formed in the ionization chamber with zero kinetic energy and falls through a potential V_1 before dissociating into an ion m_2^+ and a neutral fragment $(m_1 - m_2)$, i. e.



At the dissociation let the velocities of m_1^+ , m_2^+ and $(m_1 - m_2)$ be v_a , v_b and v_c respectively. [If the total internal energy of m_2^+ and $(m_1 - m_2)$ remained the same as that of m_1 , then $v_a = v_b = v_c$, and we should say that there was no "kinetic energy of formation" of m_2^+ .] Further, let T represent the total decrease of internal energy. Then by the law of conservation of energy

$$T + \frac{1}{2} m_1 v_a^2 = \frac{1}{2} m_2 v_b^2 + \frac{1}{2} (m_1 - m_2) v_c^2. \quad (2)$$

By the law of conservation of momentum,

$$m_1 v_a = m_2 v_b + (m_1 - m_2) v_c. \quad (3)$$

¹ J. A. HIPPLE and E. V. CONDON, Phys. Rev. **68**, 54 [1945].

² J. A. HIPPLE, R. E. FOX, and E. V. CONDON, Phys. Rev. **69**, 347 [1946].

³ A. S. NEWTON and A. F. SCIAMANNA, J. Chem. Phys. **40**, 718 [1964].